GLOBAL CHANGE BIOLOGY
BIOENERGY

GCB Bioenergy (2015), doi: 10.1111/gcbb.12272

# Crassulacean acid metabolism (CAM) offers sustainable bioenergy production and resilience to climate change

NICK A. OWEN[1], KIERAN F. FAHY[2] and HOWARD GRIFFITHS[1]

[1]*Department of Plant Sciences, Downing St. University of Cambridge, Cambridge CB2 3EA, UK,* [2]*Department of Chemistry, Imperial College London, London SW7 2AZ, UK*

## Abstract

Biomass production on low-grade land is needed to meet future energy demands and minimize resource conflicts. This, however, requires improvements in plant water-use efficiency (WUE) that are beyond conventional C3 and C4 dedicated bioenergy crops. Here we present the first global-scale geographic information system (GIS)-based productivity model of two highly water-efficient crassulacean acid metabolism (CAM) candidates: *Agave tequilana* and *Opuntia ficus-indica*. Features of these plants that translate to WUE advantages over C3 and C4 bioenergy crops include nocturnal stomatal opening, rapid rectifier-like root hydraulic conductivity responses to fluctuating soil water potential and the capacity to buffer against periods of drought. Yield simulations for the year 2070 were performed under the four representative concentration pathway (RCPs) scenarios presented in the IPCC's 5th Assessment Report. Simulations on low-grade land suggest that *O. ficus-indica* alone has the capacity to meet 'extreme' bioenergy demand scenarios (>600 EJ $yr^{-1}$) and is highly resilient to climate change (−1%). *Agave tequilana* is moderately impacted (−11%). These results are significant because bioenergy demand scenarios >600 EJ $yr^{-1}$ could be met without significantly increasing conflicts with food production and contributing to deforestation. Both CAM candidates outperformed the C4 bioenergy crop, *Panicum virgatum* L. (switchgrass) in arid zones in the latitudinal range 30°S–30°N.

*Keywords:* adaptation, *Agave tequilana*, bioenergy, CAM, climate change, Crassulacean acid metabolism, geospatial model, GIS, Nobel EPI, *Opuntia ficus-indica*, renewable energy

*Received 11 January 2015; accepted 18 April 2015*



## Introduction

Strategies to improve energy security and mitigate against the impacts of climate change commonly include the production of energy from biomass (EIA, 2013; IEA, 2013). On a calorific basis, the most important biomass resources in future energy scenarios are feedstocks specifically grown for energy (Slade *et al*., 2014). However, the utilization of land for dedicated energy crops is controversial. Conflicts that exist between land allocated to bioenergy production, food production, and biodiversity conservation have been called the 'bioenergy trilemma' (Tilman *et al*., 2009). These conflicts are predicted to become more acute with the negative impacts of climate change on water availability and food production, set against the increasing demands of a growing global population (Tilman *et al*., 2009; Godfray *et al*., 2010; Van Renssen, 2011; Creutzig *et al*., 2012; Howells *et al*., 2013; Wheeler & von Braun, 2013; Slade *et al*., 2014). One possible solution is to restrict bioenergy production to marginal and low-grade lands. Yet the extent to which such areas may be utilized remains largely unknown and would require improvements in plant water-use efficiency (WUE) that exclude most conventional C3 and C4 bioenergy crops (Somerville *et al*., 2010; Slade *et al*., 2014). In this context, we present the first global-scale geospatial productivity model for two bioenergy candidates of the highly water-use efficient crassulacean acid metabolism (CAM) pathway. We also provide an assessment of the resilience of these candidates to climate change and investigate productivity potential on low-grade lands, which we define using Food and Agriculture Organisation (FAO) land-use classifications (FAO *et al*. 2012).

Crassulacean acid metabolism has evolved on multiple occasions mostly in semi-arid, subtropical habitats and is widely considered to be an adaptation to low and intermittent water availability (Ellenberg, 1981; Ting, 1985; Winter & Smith, 1996). In contrast to the C3 and C4 metabolic pathways, CAM is characterized by the temporal separation of carboxylase activities and a four-phase carbon-uptake pattern over the diel cycle (Osmond, 1978). Phase I (PI) nocturnal atmospheric $CO_2$

Correspondence: Nick A. Owen, tel. +44 1223 333946,
email: nick.owen@cantab.net

fixation is mediated by *phosphoenolpyruvate carboxylase* (PEPC) leading to the 4C product malic acid; Phase II (PII) occurs early in the photoperiod and is defined by an overlap in PEPC and *ribulose-1, 5-bisphophate carboxylase oxygenase* (RuBisCO) activities; Phase III (PIII) occurs behind closed stomata during the photoperiod when $CO_2$ is supplied to RuBisCO from the decarboxylation of malic acid; and finally, the direct RuBisCO-mediated fixation of atmospheric $CO_2$ may occur during Phase IV (PIV) towards the end of the photoperiod under well-watered conditions (Osmond, 1978). The primary uptake of $CO_2$ at night, when temperatures are low, reduces evaporative demand across the open stomata and is a key WUE adaptation of the CAM pathway (Osmond, 1978; Smith & Nobel, 1986; Nobel, 1988; Winter & Smith, 1996). Water storage parenchyma tissue of succulent CAM species provides a buffer against periods of water deficit stress, and rectifier-like root hydraulic conductivity responses minimize retrograde plant-soil water losses and allow plants to capitalize on short periods of water availability (Barcikowski & Nobel, 1984; Smith & Nobel, 1986; Nobel, 1988).

Succulent CAM tissues allow plants to maintain water homeostasis and facilitate a carbon acquisition strategy of 'drought avoidance' (Borland *et al.*, 2011, 2014). This is distinct from 'drought tolerance', which is typically observed in arid and semi-arid C3 and C4 plants that show the capacity to endure low cell water potential or in extreme cases, desiccation (Ogburn & Edwards, 2010). Integrated over a 24-h period, typical WUE (defined as the ratio of mmol $CO_2$ fixed to mol $H_2O$ lost) values are 0.5–1.5 for C3 plants, 1.0–2.0 for C4 plants, and 4.0–10 for plants displaying CAM (Nobel, 1991). Under ideal conditions, some species of *Agave* and *Opuntia* average 43 Mg $ha^{-1}$ $yr^{-1}$ above-ground dry mass productivity which is comparable to agronomic C4 species and C3 herbaceous species and trees (Nobel, 1991). These features have lead researchers to propose that CAM plantations could be more resilient to climate change and offer higher productivity on low-grade and marginal lands than conventional C3 and C4 biomass crops (Borland *et al.*, 2009, 2014; Davis *et al.*, 2011). We tested these hypotheses by (i) constructing a global-scale geospatial productivity model for the CAM biomass candidates *Agave tequilana* and *Opuntia ficus-indica*, (ii) simulating productivity under present-day and future climate scenarios using outputs from representative concentration pathway (RCP) scenarios presented in the IPCC's 5th Assessment Report (AR5), (iii) applying macro-scale land-use constraints to estimate productivity potential on 'low-grade' lands, and (iv) comparing present-day simulations to outputs of a recently published model for the C4 biomass candidate, *Panicum virgatum* L. (switchgrass) (Kang *et al.*, 2014).

The model is based upon a refined version of the Nobel environmental productivity index (EPI) methodology, which has been validated at an agronomic scale (Nobel & Valenzuela, 1987; Nobel, 1988). Our refinements facilitate the integration of geospatial data sets to include soil water potential ($\Psi_s$) as a function of texture class and precipitation, and the capacity of CAM to buffer against periods of low $\Psi_s$. These refinements and the use of multidecadal GIS data sets to estimate, analyse, and predict productivity under various climate change scenarios are a significant advance on the initial use of the EPI approach which used point data from weather stations to predict productivity (Gracia de Cortazar & Nobel, 1990). The two candidates considered in this study, *A. tequilana* and *O. ficus-indica*, were selected for their high productivity potential (Nobel, 1991; Borland *et al.*, 2009) and favourable composition for bioenergy conversion processes over the life cycle (Yan *et al.*, 2011).

## Materials and methods

### *Refined Nobel environmental productivity index (EPI)*

CAM productivity simulations were conducted according to established Nobel EPI methodology (Nobel & Meyer, 1985; Nobel & Quero, 1986; Nobel & Valenzuela, 1987; Nobel, 1988; Garcia-Moya *et al.*, 2011) with further refinements to accommodate for spatial and temporal fluctuations in ecophysiological inputs. These include soil water retention characteristics, $CO_2$ uptake persistence during drought, and $CO_2$ uptake response to contrasting day and night temperatures.

EPI methodology states that CAM biomass productivity may be estimated by the product of three dimensionless ecophysiological response indices that quantitatively describe the effect water ($I_w$), temperature ($I_t$), and photosynthetically active radiation, PAR, ($I_p$) availability on net carbon uptake (Nobel & Valenzuela, 1987; Nobel, 1988, 1989). Ecophysiological response indices were calculated at a temporal resolution of 1 month and averaged over a 1-year period according to Eqn (1).

$$\mathrm{EPI}_{\mathrm{annual}} = \frac{\sum_{\mathrm{jan}}^{\mathrm{dec}} I_t \cdot I_w \cdot I_p}{12} \quad (1)$$

The EPI score was then multiplied by a value for maximum above-ground dry biomass productivity ($P_m$), which could occur under irrigated conditions with optimum planting-density according to Eqn (2). In this study, $P_m$ was taken as 44 and 46 Mg (dry) $ha^{-1}$ $yr^{-1}$ for *A. tequilana* (Nobel, 1988; Yan *et al.*, 2011) and *O. ficus-indica* (Nobel *et al.*, 1992), respectively. Although EPI methodology does not explicitly link plant biochemistry and physiology to productivity, the multiplication of EPI by $P_m$ implicitly takes into account agronomic scaling effects such as leaf shading.

$$P = P_m \cdot \mathrm{EPI}_{\mathrm{annual}} \quad (2)$$

Ecophysiological responses were calculated from integrated gas exchange and titratable acidity (TA) responses to changes

 doi: 10.1111/gcbb.12272

in PAR, water, and temperature (Nobel & Hartsock, 1983; Nobel & Valenzuela, 1987; Nobel, 1988; Nobel & Israel, 1994).

### *Development of ecophysiological response indices to environmental inputs*

*Ecophysiological response to water, $I_w$.* Plant water uptake is a passive process that occurs when soil water potential ($\Psi_s$) exceeds plant water potential ($\Psi_p$). $\Psi_s$ is defined as the sum of matric, osmotic, pressure, and gravitational component potentials (Campbell, 1988). Matric potential contributions are the most important determinant of $\Psi_s$ across varying soil texture classes (Cosby *et al*., 1984; Saxton *et al*., 1986; Sperry & Hacke, 2002) and occur as a result of the cohesion between water molecules and the adhesion of water molecules to the soil matrix. Water-adhesive interactions dominate the hydraulic properties of soils with high specific surface area (SSA) and result in lower measures of $\Psi_s$ at a given soil water content compared to low SSA soils (Cosby *et al*., 1984). Fine clay soils of particle diameter less than 0.002 mm have a SSA up to 840 $m^2\ g^{-1}$, whereas the SSA for gravel soils of diameter 2 mm may be as low as 0.0005 $m^2\ g^{-1}$ (Cerato & Lutenegger, 2002). Under most conditions, $\Psi_p$ fluctuates around −0.5 MPa for *Agave* and *Cacti* meaning that water uptake can occur, on average, when soil water potential ($\Psi_s$) > −0.5 MPa (Nobel, 1988).

The precipitation requirement for $\Psi_s > -0.5$ MPa was estimated for each United States Department of Agriculture (USDA) soil texture class identified in the Harmonised World Soil Database (HWSD) World Soil Atlas (see Data S1). Soil water potential was calculated as a function of soil water content ($\theta$) and texture class according to Eqn (3) (Saxton *et al*., 1986).

$$\Psi_s = A \cdot \theta^B \tag{3}$$

In Eqn (3), $A$ and $B$ are coefficients that describe soil texture contributions to $\Psi_s$ as function of sand (particle size 0.05–2.0 mm) and clay (particle size <0.002 mm) content on a mass/mass basis (Saxton *et al*., 1986). An approximation of $\theta$ at $\Psi_s = -0.5$ MPa was found for the 13 texture classes identified in USDA standards by transposing Eqn (3) to give Eqn (4).

$$\theta = (\Psi_s/A)^{(1/B)} \tag{4}$$

where

$$A = 100 \cdot \exp[a + b(\%C) + c(\%S)^2 + d(\%S)^2(\%C)]$$

$$B = e + f(\%C)^2 + g(\%S)^2 + g(\%S)^2(\%C)$$

$$a = -4.396, b = -0.0715, c = -4.88 \times 10^{-4}, d = -4.285 \times 10^{-5},$$
$$e = -3.140, f = -2.22 \times 10^{-3}, g = -3.484 \times 10^{-5}$$

Parameters used for $A$, $B$, $a$, $b$, $c$, $d$, $e$, $f$, and $g$ are given in Saxton *et al*. (1986).

Soil water potential was estimated as a function of precipitation and texture class by considering that the precipitation required to elevate $\Psi_s$ to −0.5 MPa is proportional to $\theta$ at $\Psi_s = -0.5$ MPa. Experimental data show that the relationship between days per year when $\Psi_s > -0.5$ MPa at 100–150 mm below the surface (approx. root depth of *Agave* and *Cacti*) and precipitation is approximately linear (Nobel, 1988). This allowed a gradient function ($g_i$, to be developed to estimate the duration in days when $\Psi_s > -0.5$ MPa as a function of precipitation and soil texture class, $i$. Values for $g_i$, together with soil texture characteristics, are given in Data S1. Geospatial raster files for $g_i$ were then constructed using soil texture class GIS data sets available from the HWSD (FAO *et al*. 2012) shown in Data S1. The number of days per month ($U_{\text{days}}$) when plant water uptake could occur ($\Psi_s > -0.5$ MPa) was calculated as the product of $g_i$ and precipitation according to Eqn (5) where $R$ is precipitation.

$$U_{\text{days}} = g_i \cdot R \tag{5}$$

The equations used to estimate soil water potential are valid for a wide range of textures and values of $\theta$ under unsaturated conditions (Saxton *et al*., 1986).

The value for $U_{\text{days}}$ was then scaled according to the capacities of both *A. tequilana* and *O. ficus-indica* to buffer against periods of water stress through incorporating a drought resistance factor ($F_d$). $F_d$ was taken as the fraction of carbon assimilation persistence after the onset of drought ($A_d$, $\Psi_s < -0.5$ MPa) divided by carbon assimilation under optimal conditions ($A_o$, $\Psi_s > -0.5$ MPa) integrated over 28 days according to Eqn (6).

$$F_d = 1 + \int_0^{28} A_d/A_0 \cdot \mathrm{d}t \tag{6}$$

Values for $F_d$ were calculated from TA responses to water deficit (Acevedo *et al*., 1983; Nobel & Valenzuela, 1987) and further validate against eddy covariance gas exchange data (N. Owen, unpublished data). For *A. tequilana*, $F_d$ = 1.37 dmnl and for *O. ficus-indica*, $F_d$ = 1.92 dmnl. These factors indicate that cumulative $CO_2$ uptake after 1 month of drought was 37% and 92% of uptake under optimum conditions for *A. tequilana* and *O. ficus-indica*, respectively.

The effective number of days per month ($U_e$) when plant-carbon uptake is not rate-limited by water availability was determined by Eqn (7).

$$U_e = F_d \cdot g_i \cdot R \tag{7}$$

The ecophysiological response index for water, $I_w$, was taken as the fraction of effective days where plants could uptake carbon divided by the number of days in the month ($D_m$) according to Eqn (8).

$$I_w = U_e/D_m \tag{8}$$

where $I_w = 1$ if $U_e/D_m \geq 1$

*Ecophysiological response to temperature, $I_t$.* The index for carbon-uptake response to temperature, $I_t$, was similarly determined from TA response to minimum ($t_{\min}$) and maximum ($t_{\max}$) temperature. The separation of $t_{\min}$ and $t_{\max}$ inputs was necessary because succulent CAM plants display an asymmetric sensitivity to nocturnal temperature (Nobel & Hartsock, 1978; Medina & Osmond, 1981; Buchanan-Bollig *et al*., 1984). Minimum–maximum temperature separation also allowed all combinations of day and night temperature to be used as a

 doi: 10.1111/gcbb.12272

model input. Low night temperatures facilitate carbon uptake during periods of low evaporative demand, and effect tonoplast permeability, PEPC carboxylation, and malic acid inhibition kinetics (Nobel & Hartsock, 1978; Medina & Osmond, 1981; Buchanan-Bollig *et al*., 1984; Kliemchen *et al*., 1993; Carter *et al*., 1995; Nimmo, 2000).

In a similar approach to Owen & Griffiths (2014), carbon-uptake responses to incremental changes in day–night temperature data (e.g. 10/25, 15/30, 20/35 °C) were weighted in proportion to the fraction of PI nocturnal and PII and PIII diurnal integrated gas exchange under optimal conditions. The combined temperature index, $I_t$, was taken as the average of indexes for $t_{\min}$ and $t_{\max}$. Productivity range was restricted to areas where average monthly minimum temperature >0 °C, which is consistent with the cold tolerance of both species considered (Nobel & De la Barrera, 2003; Escamilla-Treviño, 2011). Temperature response equations that are given in Eqns (9-12) were derived from TA-response data (Nobel & Valenzuela, 1987; Nobel, 1988; Nobel & Israel, 1994). The fraction of nocturnal uptake ($f_n$) and photoperiod uptake ($f_p$) are given in parentheses.

*Agave tequilana*.

$$I_{t_{\min}}(f_n = 0.87) = -0.0132t_{\min}^2 + 0.041t_{\min} - 2.18 \quad (9)$$

$$I_{t_{\max}}(f_p = 0.13) = -0.0024t_{\max}^2 + 0.146t_{\max} - 1.22 \quad (10)$$

*Opuntia ficus-indica*.

$$I_{t_{\min}}(f_n = 0.98) = -0.0041t_{\min}^2 + 0.117t_{\min} + 0.186 \quad (11)$$

$$I_{t_{\max}}(f_p = 0.02) = -0.0002t_{\min}^2 + 0.0104t_{\min} + 0.875 \quad (12)$$

The combined temperature index, $I_t$, was taken as the average of indices for $t_{\min}$ and $t_{\max}$ according to Eqn (13).

$$I_t = I_{t_{\min}}/I_{t_{\max}}, \quad \text{for } t_{\min} > 0^{\circ}\text{C} \quad (13)$$

*Ecophysiological response to photosynthetically active radiation, $I_p$*. The index for photosynthetically active radiation (PAR) was constructed from TA-response data (Nobel & Hartsock, 1983; Nobel & Valenzuela, 1987; Nobel, 1988; Nobel & Israel, 1994) normalized to 1. Equations for $I_p$ are given in Eqns (14) and (15) where PAR ($p$) is in mol $m^{-2}$ $day^{-1}$.

*Agave tequilana*.

$$I_p = -0.0007p^2 + 0.0533p + 0.0294$$
$$I_p = 1 \text{ for PAR} \geq 29 \text{ mol m}^{-2}\text{day}^{-1} \quad (14)$$

*Opuntia ficus-indica*.

$$I_p = -0.0007p^2 + 0.057p - 0.1856$$
$$I_p = 1 \text{ for PAR} \geq 35 \text{ mol m}^{-2}\text{day}^{-1} \quad (15)$$

*Input data sets and data processing*. Ecophysiological response indices were developed according to Eqns 3–15 using $CO_2$ gas exchange and titratable acidity data presented in Nobel & Hartsock (1983), Nobel & Valenzuela (1987), Nobel (1988), Nobel & Israel (1994), and Acevedo *et al*. (1983).

WorldClim data averaged over the period 1950–2000 was used to estimate current productivity (WorldClim, 2014). Productivity in the year 2070 ($P_{2070}$) was forecasted using output averaged over the period 2061–2080 from all global climate models (GCMs) models cited in the IPCCs 5th Assessment Report (IPCC *et al*., 2013; WorldClim, 2014). Geospatial inputs for PAR were estimated from National Aeronautics and Space Administration (NASA) data sets for monthly 'Insolation Incident On A Horizontal Surface' (kWh $m^{-2}$ $day^{-1}$) averaged over a 22-year period (July 1983–June 2005) (NASA, 2014). PAR (mol $m^{-2}$ $day^{-1}$) was estimated from solar insolation ($I_s$ in kWh $m^{-2}$ $day^{-1}$) by assuming that 48% of solar energy falls within the PAR range of 400–700 nm (Britton & Dodd, 1976) and a solar radiation to photon flux conversion coefficient of 4.57 mol photons $MJ^{-1}$ (Amthor, 2010). Data were resampled to 0.1 decimal degrees (DD) using cubic convolution interpolation. World soil texture class data were sourced from the HWSD (FAO *et al*. 2012).

Sustainable biomass standards set out by the Global Bioenergy Partnership (GBEP), the Roundtable on Sustainable Biomaterials (RSB), and the Renewable Energy Directive 2009/28/EC of the European Union were use as a guide to develop macro-scale geospatial constraints to estimate low-impact biomass potential (GBEP, 2011; RSB, 2013). It should be noted that criteria set out by sustainable bioenergy initiatives also commonly include localized factors such as subsistence farming land use, economic viability, and cultural importance (Scarlat & Dallemand, 2011; Dauber *et al*., 2012). These considerations were beyond the scope of the macro-scale evaluation presented here. The definition of low-grade lands adopted in this study excludes forests, protected areas, wetlands, and highly productive and irrigated agricultural lands. These lands were identified using United Nations Food and Agriculture Organisation (FAO) geospatial land-use data and classifications (Nachtergaele & Petri, 2008). A world map of 'low-grade' lands according to our definition, as well FAO land-use patterns, is given in Data S2. Commercially viable yields were considered to exceed 5 Mg $ha^{-1}$ $yr^{-1}$ and assumed to have a dry biomass energy content of 18 GJ $Mg^{-1}$ (Slade *et al*., 2014).

Simulated data for switchgrass productivity presented in Kang *et al*. (2014) were provided by Dr Shujiang Kang. Geospatial data sets were processed using ArcGIS software version 10.1 (ESRI, 2012) at a spatial resolution of 0.1 decimal degrees.

## Results

### *Global biomass yield*

World productivity simulations under 20th century conditions for (a) *A. tequilana* and (b) *O. ficus-indica* are given in Fig. 1. Productivity ranged from 0.0 to 38.0 (EPI, 0.0–0.86) and 0.0 to 40.0 Mg (dry) $ha^{-1}$ $yr^{-1}$ (EPI, 0–0.87) for *A. tequilana* and *O. ficus-indica*, respectively. As neither candidate achieved maximum theoretical

 doi: 10.1111/gcbb.12272

yield (EPI = 1), these results show that carbon uptake was rate-limited by the seasonal availability of either (or combination of) water, temperature, and PAR in all parts of the World at some time throughout the year. In general, simulations show that *O. ficus-indica* displays an extended range of high productivity (>50% $P_m$) compared to *A. tequilana*. This can be seen across arid and semi-arid regions in Australia, East India, sub-Saharan Africa, and the southern United States. The productive range of both candidates is restricted to the minimum monthly temperature isotherm of 0 °C, which is consistent with the cold tolerance of both species.

Although *O. ficus-indica* generally achieves higher productivity than *A. tequilana* (max. 40 vs. 38 Mg (dry) $ha^{-1}$ $yr^{-1}$) and better yield distribution, the higher water-soluble carbohydrate composition of *A. tequilana* is more suitable for bioethanol conversion processes (Stintzing & Carle, 2005; Li *et al.*, 2012). Therefore, in areas where both candidates produce significant yields, the decision of which to cultivate may in large part be determined by the intended application.

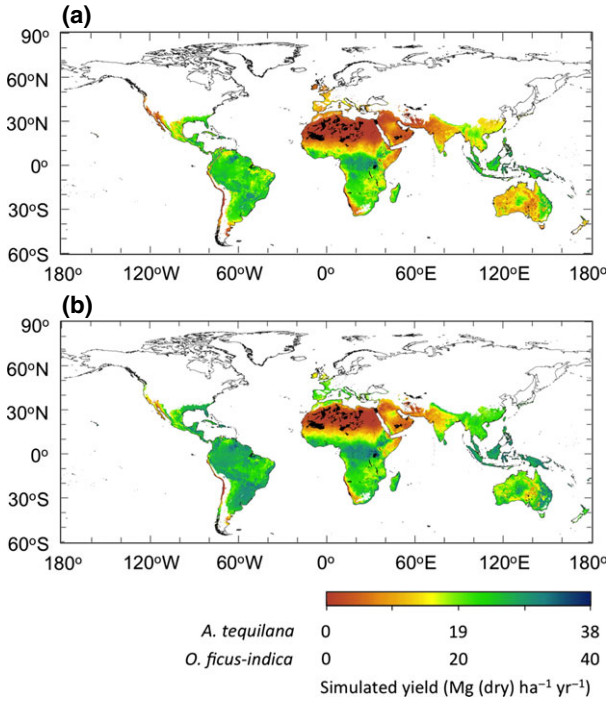


**Fig. 1** World productivity simulations for (a) *Agave tequilana* and (b) *Opuntia ficus-indica* under current climate conditions (1950–2000). Areas of high productivity for *A. tequilana* are comparatively more restricted than for *O. ficus-indica*. This is due to the higher sensitivity to minimum temperature and a reduced capacity of *A. tequilana* to buffer against low soil water potential ($F_d$). The higher PAR requirement of *O. ficus-indica* compared to *A. tequilana* (35 and 29 mol $m^{-2}$ $day^{-1}$, respectively) has a negative impact on yields outside 30°S–30°N. For both species, the productive range is restricted to areas where $t_{min}$ > 0 °C.

Raster file EPI data of Fig. 1 that are unscaled with $P_m$, are available for download in Data S5 and S6. These maps can be viewed, refined, or rescaled with different values for $P_m$ as desired using ArcGIS software (see Data S4 for instructions).

### *Resilience to climate change*

Productivity simulations were performed in the year 2070 under the representative concentration pathway (RCP) scenarios defined in the IPCC's Fifth Assessment Report (AR5). The impacts of climate change were evaluated in terms of change in geospatial and latitudinal productivity distribution, total yield, and the distance that the mean of the latitudinal productivity distribution migrates relative to the equator under 70RCP2.6-8.5 (Figs 2 and 3). The RCPs consider radiative forcing scenarios of 2.6, 4.5, 6.0, and 8.5 W $m^{-2}$ relative to pre-industrial levels by the year 2100 (WorldClim, 2014). The best case scenario is RCP 2.6 (70RCP2.6), and the worst case scenario is RCP 8.5 W $m^{-2}$ (70RCP8.5).

Simulated change in productivity relative to the present for each RCP scenario is given in Fig. 2. Note that percentage change in yield has been given relative to the present, and error is more significant in areas that currently support very low yields, such as North Africa. Also, while Fig. 2a,b shows that productivity is likely to decline in many areas relative to the present, forecasts relative to the 'best case' 70RCP2.6 suggest a higher capacity for resilience. Climate scenario evaluations against the 'locked-in' best case (between 70RCP2.6 and 70RCP8.5) have been provided in Fig. 2c,d as these simulations may be more applicable to inform policymakers.

Under RCPs 70RCP2.6-6.0, productivity losses for *A. tequilana* range from −5 to −25% in equatorial regions with isolated areas of resilience and higher productivity restricted to mountain ranges that allow progressive altitudinal migration to locations with lower night temperatures. Outside the latitudinal range of 25°S–25°N, productivity is likely to increase under 70RCP2.6-6.0. The worst case 70RCP8.5 scenario may result in significant losses of >25% in equatorial regions extending to 30°S–30°N. *Opuntia ficus-indica* shows greater resilience to climate change with losses restricted to −5% to −15% under 70RCP2.6-6.0 across all productive areas and increasing to −25% to −15% in equatorial regions under 70RCP8.5. For *A. tequilana*, higher night temperatures generally improve yields outside latitudes of 30°S–30°N, but have a negative impact within this latitudinal range. Higher night temperatures extend the productivity range of both species, although suboptimal conditions in these fringe regions only sup-

 doi: 10.1111/gcbb.12272

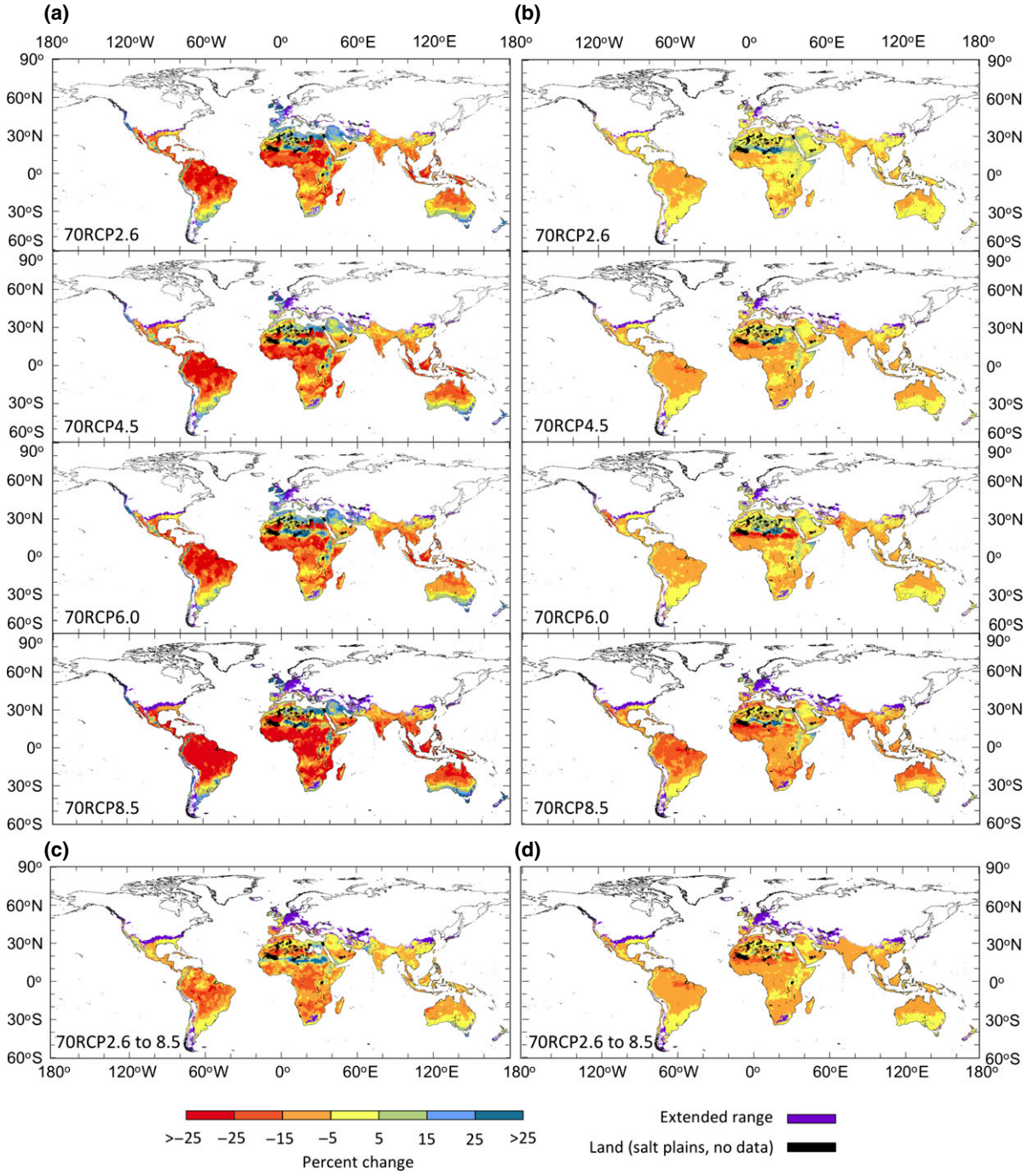


**Fig. 2** Simulated change in productivity under IPCC RCP climate change scenarios. Simulations show the change in productivity in the year 2070 under IPCC climate change scenarios relative to present yields (1950–2000) for (a) *Agave tequilana* and (b) *Opuntia ficus-indica*. Change in yield between the best case scenario (70RCP2.6) relative to worst case scenario (70RCP8.5) in the 2070 is shown in (c) for *A. tequilana* and (d) for *O. ficus-indica*. The area of extended range (purple) is determined by the minimum isotherm, $t_{min} > 0$ °C. Geospatial yield patterns show that for both *A. tequilana* and *O. ficus-indica*, the greatest losses are most likely in equatorial regions, with both candidates displaying considerable resilience under 70RCP4.5 and 70RCP6.0 relative to the minimum best case scenario 70RCP2.6. Climate change scenario 70RCP8.5 is likely to have significant negative impacts on yields for both candidates in the latitudinal range 30°S–30°N. Outside this range, yields are likely to increase for *A. tequilana* under all RCPs and remain approximately the same for *O. ficus-indica*. A comparison between the best case 'locked-in' scenario 70RCP2.6 with the worst case 70RCP8.5 for *A. tequilana* (c) and *O. ficus-indica* (d) shows considerable resilience even though climate change will have a progressively more negative impact on yield.

 doi: 10.1111/gcbb.12272

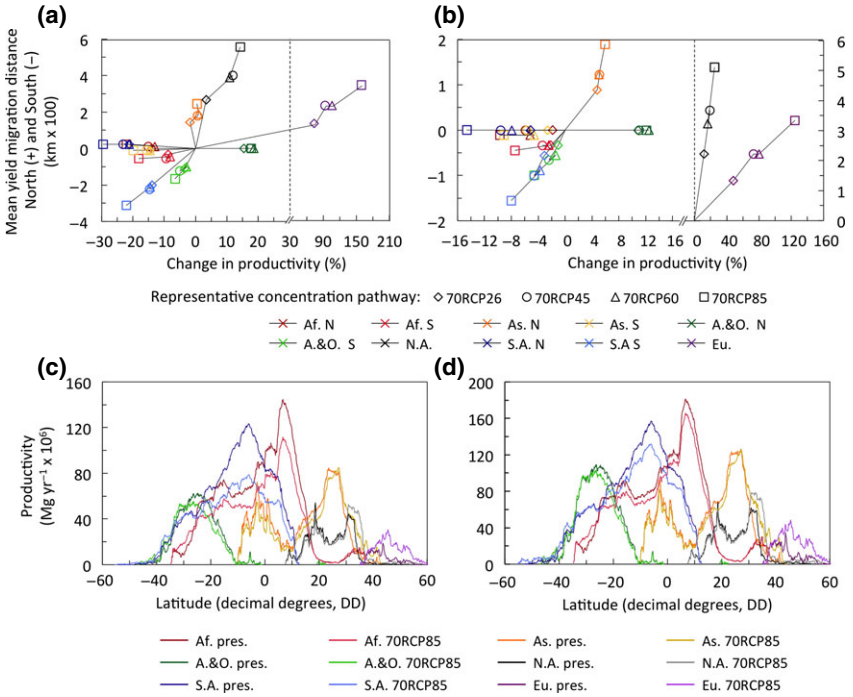


**Fig. 3** Climate change impacts on productivity distribution. Continent-scale analysis of climate change impacts on total yield and migration of mean yield in the year 2070 under IPCC RCP scenarios for (a) *Agave tequilana* and (b) *Opuntia ficus-indica*. Continents are divided into areas north and south of the equator to analyse yield migration, where the present is coordinates 0, 0 (no change) in (a, b). *Opuntia ficus-indica* has potential for stronger resilience to climate change compared to *A. tequilana* based on measures for total yield and degree of yield migration from the equator. Histograms show the change in latitudinal yield distribution between the present and worst case climate change scenario (70RCP8.5) for (c) *A. tequilana* and (d) *O. ficus-indica*. In general, the histograms show a tendency for migration towards the poles for both candidates. Abbreviations: Africa north (Af. N), Africa south (Af. S), Asia north (As. N), Asia south (As. S), Australia and Oceania north (A.&O. N), Australia and Oceania south (A.&O. S), North America (N.A.), South America north (S.A. N), South America south (S.A. S), Europe (Eu.).

port low productivity. Compared to *O. ficus-indica*, *A. tequilana* exhibits greater sensitivity to climate change with greater productivity losses in equatorial regions and greater gains outside latitudes of 25°S–25°N.

Relative to the best case 70RCP2.6 scenario, however, the outlook is significantly more positive. For *A. tequilana*, 2070 simulations remain relatively constant under 70RCP4.5-6.0. *Opuntia ficus-indica* is highly resilient under all climate change scenarios relative to 70RCP2.6, with moderate −5% to −15% losses occurring in some equatorial areas under 70RCP8.5. For both candidates, the greatest losses are associated with higher minimum night temperature and altered precipitation patterns in tropical and subtropical zones. These areas, that are the most vulnerable to the negative impacts of climate change, are mostly excluded from the analysis of low-grade land yields given below.

Continental-scale climate impacts are considered in Fig. 3a-d. Continents were divided into regions north and south of the equator to investigate yield migration patterns and changes in total productivity under the IPCC climate scenarios. The landmass of Africa north of the equator (Af.N) displayed strong migration resilience for both candidates although productivity is likely to decline by 15–20% and 2–10% for *A. tequilana* and *O. ficus –indica*, respectively, for 70RCP2.6-8.5. Areas of Africa south of the equator (Af.S) show considerable resilience with mean yields migrating 30–50 km south for both candidates and decreasing by 10–20% for *A. tequilana* and 2–8% for *O. ficus-indica*. Productivity in Asia north of the equator (As.N) is likely to remain constant for *A. tequilana* and increase by 5–6% for *O. ficus-indica*, while mean yields migrate by 150–250 and 90–200 km north, respectively, for scenarios 70RCP2.6-8.5. In Asia south (As.S), productivity is likely to decrease by 20% for *A. tequilana* and 10% for *O. ficus-indica* with mean yield migration staying relatively constant. Simulations for Australia and Oceania south (A.&O.S) indicate significant productivity resilience although mean yields are likely to migrate 100–160 km for *A. tequilana* and 30–90 km south for *O. ficus-indica*. Australia and Oceania north (A.&O.N) consists of Pacific Islands with restricted land area and relatively limited productivity potential. For North America (N.A.) and Europe (Eu.),

 doi: 10.1111/gcbb.12272

large migration distances are accompanied by significant increases in yield, which is attributed to the extended range where both candidates may be cultivated due to elevated average minimum temperatures. In terms of yield, potential, and migration, the most detrimental effects of climate change are likely to be observed in South America.

Latitudinal productivity distribution under present conditions and 70RCP8.5 (Fig. 3c-d also indicate that climate change is likely to have a beneficial impact at latitudes outside 30°S–30°N for *A. tequila* and outside 25°S–25°N for *O. ficus-indica*. Mean yields are likely to migrate towards the poles for both candidates. Based on the simulations shown in Fig. 2, O. *ficus-indica* is consistently more resilient to the impacts of climate change than *A. tequilana*.

## Discussion

In this section, the impact of ecophysiological responses on yield distribution is discussed with the aid of the sensitivity analysis presented in Fig. 4. Sources of uncertainty and key assumptions are then identified and discussed. Productivity simulations for both CAM candidates are then compared to a recently published model of the C4 bioenergy candidate, *Panicum virgatum* L. (switchgrass). Finally, commercially viable and macro-scale sustainability constraints are applied to outputs presented in Fig. 1 to estimate viable low-grade land (VL) yield potential.

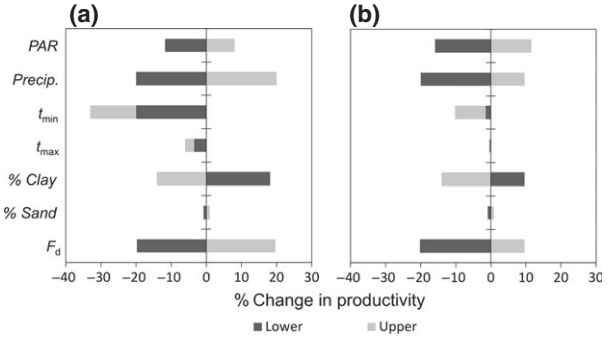


**Fig. 4** Sensitivity analysis of key input parameters. The sensitivity analysis for (a) *Agave tequilana* and (b) *Opuntia ficus-indica* shows the effect of changing key input parameters on simulated productivity. The range of the sensitivity analysis for each parameter is shown in the parentheses (lower, middle, upper) as follows: photosynthetically active radiation *PAR* (20, 25, 30 mol $m^{-2}$ $day^{-1}$); precipitation (40, 50, 60 mm $month^{-1}$); average minimum temperature, $t_{min}$: *A. tequilana* (10, 15, 20 °C), *O. ficus-indica* (11, 16, 21 °C); average maximum temperature, $t_{max}$: *A. tequilana* (25, 30, 35 °C), *O. ficus-indica* (21, 26, 31 °C); % clay (28, 35, 42); % sand (28, 35, 42); drought-buffering factor, $F_d$: *A. tequilana* (1.10, 1.37, 1.64 dmnl), *O. ficus-indica* (1.54, 1.93, 2.32 dmnl).

### *Ecophysiological responses and yield distribution*

Figure 1 shows that *O. ficus-indica* is likely to have a more extensive range of high productivity potential (EPI > 0.5) than *A. tequilana*. This is attributed to the comparatively greater capacity to buffer against periods of low soil water potential (described by factor, $F_d$) and lower sensitivity to minimum temperature ($t_{min}$). For the conditions defined in the sensitivity analysis in Fig. 4, increasing $F_d$ by 20% results in an approx. 20% and 10% increase in carbon uptake for *A. tequilana* and *O. ficus-indica*, respectively. This shows that an increase in $F_d$ would benefit *A. tequilana* more than *O. ficus-indica*. The greater capacity of *O. ficus-indica* to buffer against water deficit also meant that a 20% increase in precipitation has a smaller positive impact on yield than for *A. tequilana* in areas that receive approx. 50 mm of precipitation per month. These results suggest that, although both plants show reasonably strong resilience to climate change, the amount and temporal distribution of precipitation patterns could have a significant impact on yields.

Soil clay content, which by extension determines soil water potential according to Eqn (4), also has a significant and similar effect on yield as precipitation. A reduction in soil clay content had a more positive impact on simulated productivity for *A. tequilana* compared to *A. ficus-indica* due to this plants comparatively lower capacity to buffer against low $\Psi_s$. The impact of clay content on yield, together with soil texture information given in Data S1, indicate that soil properties are a dominant factor determining productivity at a localized scale. In areas where Type 13 clayey soils (75% clay) border Type 1 sandy soils (5% clay), for example, simulated productivity may decrease by up to 80%. As the water-uptake threshold for both species occurs at the same soil water potential ($\Psi_s = -0.5$ MPa (Nobel, 1988)), differences in water relations were determined by $F_d$ rather than plant-soil uptake relations.

The sensitivity analysis in Fig. 4 shows that *O. ficus-indica* is significantly more resilient to deviations from the optimum minimum night temperature than *A. tequilana*. For example, a deviation of 5 °C from the optimum reduces simulated yields by 20–33% for *A. tequilana* compared to a reduction of 2–12% for *O. ficus-indica*. In general, the negative impacts of climate change in equatorial regions are mostly attributed to high suboptimal $t_{min}$. At latitudes outside 30°S–30°N, higher $t_{min}$ has a strong positive impact on yield for *A. tequilana*. However, a recent study on *Agave angustifolia* showed strong commitment to CAM and high $CO_2$

 doi: 10.1111/gcbb.12272

uptake persistence over a wide range of day and night temperatures (Holtum & Winter, 2014). The results of this study suggest that *Agave* species that inhabit tropical regions, with characteristically higher nocturnal temperatures, could be more suitable for biomass production in warmer equatorial climates.

Data used to construct the ecophysiological response index to PAR show that carbon-uptake response saturates at 35 mol $m^{-2}$ $day^{-1}$ for *O. ficus-indica*, higher than for *A. tequilana* at 29 mol $m^{-2}$ $day^{-1}$ (Nobel & Hartsock, 1983; Nobel & Valenzuela, 1987). This has a small negative impact on *O. ficus-indica* productivity outside latitudes of 30°S–30°N.

### *Uncertainty and key assumptions*

Four categories of potential error were identified: input data sets, methodology, key assumptions, and exclusions. Input data sets include global climate models (GCMs), the harmonized world soil database (HWSD) texture data, solar radiation data, and land-use constraints. To minimize error from GCM inputs, the mean output of all GCMs referenced in the IPCC's 5th Assessment Report averaged over the period 2061–2080 was used to generate forecasts for the year 2070. GIS soil data sets were resolved into 13 categories according to USDA standards to minimize error from soil texture inputs. It should be noted that simulations are subject to the sparsity of data and interpolation methods used to construct all geospatial input data sets (see referenced data for information on input data set limitations).

Methodological error may include error associated with the EPI approach, the use of titratable acidity (TA) to derive ecophysiological response indices, and the scaling of EPI with a value of maximum dry biomass productivity ($P_m$). Although the Nobel EPI approach has been validated against biomass accumulation and leaf-unfurling rates in the field (Nobel & Valenzuela, 1987; Nobel, 1988, 1989), further validation across contrasting environmental conditions would be desirable. The use of TA as proxy to estimate carbon uptake is based on the 1 : 2 : 1 stoichiometric relationship between nocturnal $CO_2$ fixation, $H^+$ and 4C product, malic acid (Osmond, 1978). It should be noted, however, that ΔTA-based approaches do not account for PIV carbon uptake and PI refixation of respiratory $CO_2$ and could therefore be prone to error. In the case of *A. tequilana* and *O. ficus-indica*, PIV only accounts for approximately 13% and 2% of integrated daily carbon uptake, respectively, under optimal conditions (derived from data presented in Nobel & Valenzuela (1987) and Nobel & Israel (1994)). Additionally, a recent agronomic-scale eddy covariance (EC) gas exchange study over a field of *A. tequilana* (N. Owen, unpublished data) showed that whole-plant averaged ΔTA measurements closely agreed with integrated daily gas exchange after 70 days of drought. The EC data support the use of ΔTA as a proxy for carbon uptake as contributions from recycled respiratory $CO_2$ refixation in PI (that contributes to ΔTA) seem to approximately equate to Phase IV $CO_2$ uptake (which is not measured in ΔTA measurements) overall under field conditions.

The values adopted for $P_m$ used to scale EPI to estimate actual productivity may also contribute error. Under the relatively low planting densities employed by current commercial applications (food and alcohol production), $P_m$ is approx. 25 and 18–20 Mg (dry) $ha^{-1}$ $yr^{-1}$ for *Agave* and *Opuntia* species, respectively. However, under optimal planting densities reported, $P_m$ is significantly higher, at 38 and 47 Mg (dry) $ha^{-1}$ $yr^{-1}$, respectively, (Nobel, 1991). As $P_m$ is dependent on cultivation practices employed, unscaled EPI maps have been provided in Data S5 and S6 which may be rescaled with a chosen value of $P_m$ as desired.

Two key assumptions were required to integrate geospatial data sets with plant ecophysiological response data. Firstly, the continuum of night–day temperatures was incorporated by making the assumption that minimum temperature sensitivity is proportional to nocturnal carbon uptake and that maximum temperature sensitivity is proportional to photoperiod uptake of $CO_2$. This assumption was based on the well established hypersensitivity of succulent CAM species to night temperature for the species considered (Nobel, 1976; Nobel & Hartsock, 1978; Medina & Osmond, 1981; Acevedo *et al.*, 1983; Grams *et al.*, 1997; Borland *et al.*, 1999). However, a recent study on *Agave antustifolia* that showed high resilience to temperature suggests that this approach is most likely conservative (Holtum & Winter, 2014). Secondly, the duration for which $\Psi_s$ was greater than $\Psi_p$ was benchmarked against measured data sets showing linear relationships between precipitation and the duration for which $\Psi_s > -0.5$ MPa (Nobel, 1988).

Exclusions from the model include soil-nutrient inputs, species invasiveness, fertilization effects of high atmospheric $CO_2$ concentration, and plant-acclimation capacity. The latter two are likely to improve CAM yields (Nobel & Israel, 1994).

### *Comparison between CAM candidates and the C4 bioenergy candidate, Panicum virgatum L (switchgrass)*

A geospatial comparison between simulated output for *A. tequilana* and *O. ficus-indica* with the outputs of a recently published model of *Panicum virgatum* L. (switchgrass) productivity (Kang *et al.*, 2014) is given in Fig. 5. *Panicum virgatum* L. is a perennial C4 bioenergy

 doi: 10.1111/gcbb.12272

candidate that has demonstrated high productivity potential over contrasting nutrient, temperature, and water availability regimes (Sanderson *et al.*, 1996; Keshwani & Cheng, 2009). In Fig. 5, only 'commercially viable' yields of ≥5 Mg (dry) $ha^{-1}$ $yr^{-1}$ are considered. In general, simulations show that *P. virgatum* L. achieves higher productivity than both CAM candidates in regions outside the latitudinal range of 30°N–30°S. Inside this latitudinal range, however, *A. tequilana* outperformed *P. virgatum* L. with the exception of parts of equatorial South America, Africa where *A. tequilana* yields are negatively impacted by high average monthly minimum temperature, $t_{min}$ (see Fig. 4). *O. ficus-indica* generally outperformed *P. virgatum* L. in almost all areas inside 30°N–30°S with the exception of restricted parts of the wet tropics and northern China where simulated yields were similar (<25% difference).

The different yield-distribution patterns reflect the different carbon acquisition strategies of arid and semi-arid perennial grasses compared to succulent CAM species. Herbaceous perennials such as *P. virgatum* L. have a short growth season that is restricted to warm and wet months from a rootstock that becomes dormant over a dry season or winter period (Skinner & Adler, 2010). These traits allow significant levels of productivity to extend to areas that experience harsh winter conditions at latitudes up to 55°N. On the other hand, *O. ficus-indica* and *A. tequilana* grow throughout the year and are highly sensitive to $t_{min}$. The higher productivity potential of both CAM species in arid and semi-arid areas inside the latitudinal range of 30°N–30°S is mostly attributed to rectifier-like root hydraulic conductivity responses that allow plants to capitalize on low and infrequent precipitation events. These hydraulic responses also allow the recharge of water storage parenchyma which supports continued physiological and metabolic function during extended periods of drought ($\Psi_s < -0.5$ MPa). The results presented here suggest that the different strategies employed by succulent CAM species, compared to C4 grasses, are likely to translate to higher productivity potential in tropical areas of low rainfall.

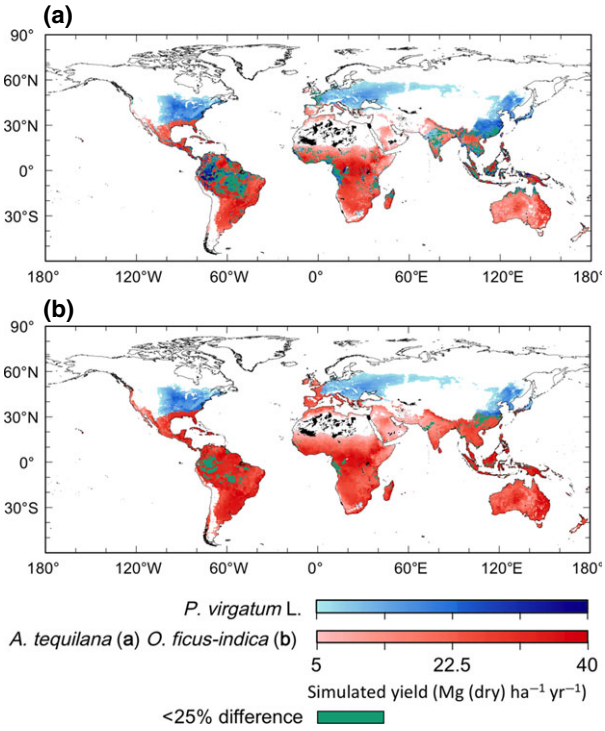


**Fig. 5** Comparison of CAM bioenergy candidates *A. tequilana* (a) and *O. ficus-indica* (b) with the C4 bioenergy crop *P. virgatum* L (switchgrass). Simulations show that both CAM candidates generally outperform *P. virgatum* over the latitudinal range 30°S–30°N. Higher seasonal variation in temperature outside this range and in mountainous areas tend to favour *P. virgatum* L. In the wet tropics, *P. virgatum* L. and *A. tequilana* display similar yield potential (<25% difference). Only 'commercially viable' yields ≥5 Mg (dry) $ha^{-1}$ $yr^{-1}$ are shown.

### *Viable low-grade land yield potential*

Exploiting the bioenergy potential of the CAM pathway in a sustainable manner is contingent upon feedstock cultivation on low-grade land. However, there are no standard definitions for classes of 'surplus' land, which are a function of subsistence farming land use, economic viability, cultural importance, and biodiversity value (Dauber *et al.*, 2012). Such lands must be evaluated at a local scale (Dauber *et al.*, 2012; Immerzeel *et al.*, 2014) and to our knowledge no global-scale geospatial data sets that identify categories of surplus land are available. We therefore elected to define 'viable low-grade' lands (VL) using present-day Food and Agriculture Organisation (FAO) (Nachtergaele & Petri, 2008) land-use classifications. As initial land use is a major determinant of the environmental performance of dedicated bioenergy crops (Immerzeel *et al.*, 2014), areas of high and irrigated agricultural activity, forests, and protected areas were excluded (refer to Data S2 for a list of FAO constraints used). To enable direct comparison with a review of global biomass energy resources, viable yields were considered to exceed 5 Mg $ha^{-1}$ $yr^{-1}$ and assumed to have a dry biomass energy content of 18 GJ $Mg^{-1}$ (Slade *et al.*, 2014). Therefore, VL maps in Fig. 6 illustrate yields that are theoretically possible on 'low-grade lands' at a global scale, without accounting for local social acceptability or environmental impacts. ASCII files for Fig. 6 have been provided in the Data S7 and S8 to enable adjustment or refinement of the land-use constraints as desired using GIS software.

 doi: 10.1111/gcbb.12272

Simulations presented in Fig. 6 suggest that VL yields are highly resilient to climate change and may have the capacity to meet 'extreme' (Slade *et al.*, 2014) future bioenergy demands of >600 EJ $yr^{-1}$. Once again comparing the 70RCP8.5 to the present, climate change may have a positive impact on VL yields in Asia (+3.6%), Europe (+165%), and North America (+18%) for *A. tequilana*. Similarly, for *O. ficus-indica*, climate change may have a positive impact in Asia (+8.8%), Europe (+132%) North America (+28%), and South America (+0.1%). See Data S3 for simulation data presented in the barcharts in Fig. 6.

Compared to the present, 70RCP8.5 world VL yields may decrease by −11% (497–444 EJ) for *A. tequilana* but remained fairly constant for *O. ficus-indica* at −1% (756–750 EJ). The land area that supports these yields, shown in Fig. 6, is 1950 Mha (av. 14.2 Mg $ha^{-1}$ $yr^{-1}$) for *A. tequilana* and 2300 Mha (av. 18.3 Mg $ha^{-1}$ $yr^{-1}$) for *O. ficus-indica*. Similarly under 70RCP8.5, VL yields for *A. tequilana* and *O. ficus-indica* may be produced on 2070 Mha (av. 11.9 Mg $ha^{-1}$ $yr^{-1}$) and 2510 Mha (av. 16.6 Mg $ha^{-1}$ $yr^{-1}$), respectively. For context, this represents 13.9% and 16.8% of the world's terrestrial land area, respectively. These results suggest that climate change will have a small overall negative impact on world VL yield intensity.

A bioenergy review by Slade *et al.* (2014) found that dedicated bioenergy crops may contribute 22–1272 EJ by 2050 (Slade *et al.*, 2014). The authors considered scenarios >600 EJ $yr^{-1}$ as 'extreme' and based on assumptions that increases in food-crop yields will significantly outpace demand, 1000 Mha of high-grade agricultural land will be available for bioenergy, population growth will be low, a primarily vegetarian diet will be adopted, and extensive deforestation would be allowed to continue (Slade *et al.*, 2014). For context, current world bioenergy demand is approximately 50 EJ $yr^{-1}$ and represents 10% of total world energy demand (IEA, 2013). Significantly, the theoretical results presented here show that VL land yields for *O. ficus-indica* could meet these extreme bioenergy demand scenarios (>600 EJ $yr^{-1}$) without requiring

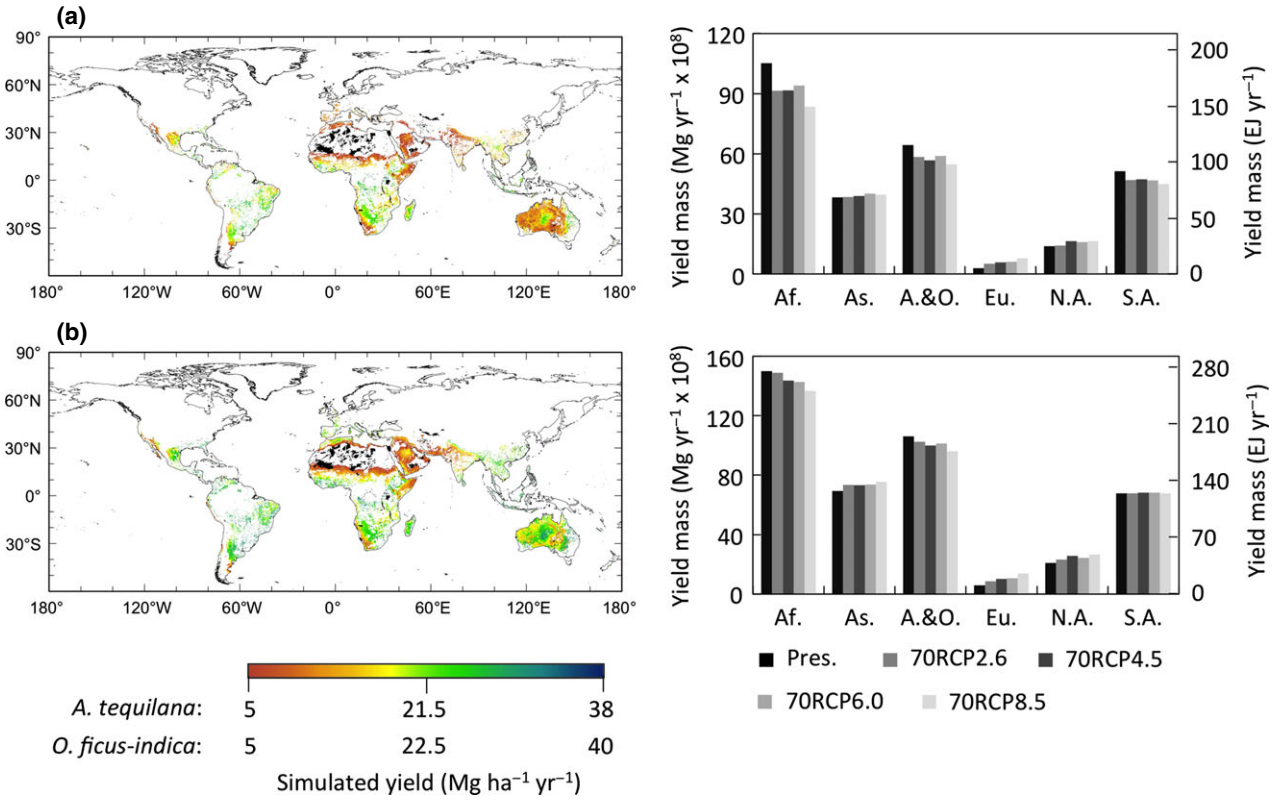


**Fig. 6** Viable low-grade land (VL) productivity potential under IPCC RCP climate change scenarios. The geospatial productivity simulations show VL yields under current climate conditions (1950–2000) and the barcharts give total VL productivity under each RCP scenario in the year 2070 for each continent for (a) *A. tequilana* and (b) *O. ficus-indica*. VL yields for were constrained to ≥5 Mg $ha^{-1}$ $yr^{-1}$ and exclude highly productive and irrigated agricultural lands, forests, and protected areas. Simulations for *A. tequilana* show that climate change will have a positive impact in Asia, Europe, and North America. For *O. ficus-indica*, climate change may have a positive impact in Asia, Europe, North America, and South America. Large expanses of Saharan Africa, the Middle East, and Australia were excluded due to the commercially viable yield requirement of ≥5 Mg $ha^{-1}$ $yr^{-1}$.

additional high-grade agricultural land and will continue to do so under the worst case climate change scenario. However, while these results underscore the high productivity potential of *O. ficus-indica*, we do not suggest such large-scale development would be environmentally or socially desirable, or practically feasible.

The model simulations presented here indicate that CAM bioenergy candidates are likely to outperform C3 and C4 bioenergy crops in terms of low-grade land productivity and meeting sustainable bioenergy objectives. Features including nocturnal carbon uptake, rectifier-like root hydraulic conductivity responses to fluctuating $\Psi_s$, and the capacity to buffer against periods of water deficit stress allow high productivity rates on low-grade lands. The yield simulations highlighted the capacity of the CAM pathway to meet future bioenergy demands with minimum resource conflicts. The same WUE features of the CAM pathway that distinguish it from C3 and C4 bioenergy candidates also offer resilience to climate change. Low-grade land simulations comparing the worst case climate scenario (70RCP8.5) with present suggest that total yield will fall by 11% for *A. tequilana* and remain approximately unchanged for *O. ficus-indica* in 2070. However, CAM biofuels are not exempt from criticisms made of first generation C3 and C4 bioenergy candidates. While the macro-scale analysis presented here provides a good approximation of CAM bioenergy potential on a global scale, the sustainable introduction of CAM crops will need to be evaluated on a case-by-case basis and in accordance with sustainable bioenergy standards.

## Acknowledgements

The authors would like to thank Dr Jessica Royles, Dr Moritz Meyer, and Jamie Males for their help and advice. Thanks also to Dr Shujiang Kang (Oak Ridge Laboratory, TN USA) for providing simulated output from his recent switch grass global productivity model. This research is funded by the Australian Rural Industries Research and Development Corporation (RIRDC).

## References

Acevedo E, Badilla I, Nobel PS (1983) Water relations, diurnal acidity changes, and productivity of a cultivated cactus, *Opuntia ficus-indica*. *Plant Physiology*, **72**, 775–780.

Amthor JS (2010) From sunlight to phytomass: on the potential efficiency of converting solar radiation to phyto-energy. *The New Phytologist*, **188**, 939–959.

Barcikowski W, Nobel PS (1984) Water relations of *Cacti* during desiccation: distribution of water in tissues. *Botanical Gazette*, **145**, 110–115.

Borland AM, Hartwell J, Jenkins GI, Wilkins MB, Nimmo HG (1999) Metabolite control overrides circadian regulation of *Phosphoenolpyruvate Carboxylase Kinase* and $CO_2$ fixation in crassulacean acid metabolism. *Plant Physiology*, **121**, 889–896.

Borland AM, Griffiths H, Hartwell J, Smith JAC (2009) Exploiting the potential of plants with crassulacean acid metabolism for bioenergy production on marginal lands. *Journal of Experimental Botany*, **60**, 2879–2896.

Borland AM, Zambrano VAB, Ceusters J, Shorrock K (2011) The photosynthetic plasticity of crassulacean acid metabolism: an evolutionary innovation for sustainable productivity in a changing world. *The New Phytologist*, **191**, 619–633.

Borland AM, Wullschleger SD, Weston DJ, Hartwell J, Tuskan GA, Yang X, Cushman JC (2014) Climate-resilient agroforestry: physiological responses to climate change and engineering of crassulacean acid metabolism (CAM) as a mitigation strategy. *Plant, Cell & Environment*, 1–17. doi: 10.1111/pce12479.

Britton CM, Dodd JD (1976) Relationships of photosynthetically active radiation and shortwave irradiance. *Agricultural Meterology*, **17**, 1–7.

Buchanan-Bollig IC, Kluge M, Müller D (1984) Kinetic changes with temperature of *phosphoenolpyruvate carboxylase* from a CAM plant. *Plant, Cell & Environment*, **7**, 63–70.

Campbell GS (1988) Soil water potential measurement: an overview. *Irrigation Science*, **9**, 265–273.

Carter PJ, Wilkins MB, Nimmo HG, Fewson CA (1995) Effects of temperature on the activity of *phosphoenolpyruvate carboxylase* and on the control of $CO_2$ fixation in *Bryophyllum fedtschenkoi*. *Planta*, **196**, 375–380.

Cerato AB, Lutenegger AJ (2002) Determination of surface area of fine-grained soils by the ethylene glycol monoethyl ether. *Geotechnical Testing Journal*, **25**, 315–321.

Cosby BJ, Hornberger GM, Clapp RB, Ginn TR (1984) A statistical exploration of the relationships of soil moisture characteristics to the physical properties of soils. *Water Resources Research*, **20**, 682–690.

Creutzig F, Popp A, Plevin R, Luderer G, Minx J, Edenhofer O (2012) Reconciling top-down and bottom-up modelling on future bioenergy deployment. *Nature Climate Change*, **2**, 320–327.

Dauber J, Brown C, Fernando AL *et al.* (2012) Bioenergy from "surplus" land: environmental and socio-economic implications. *Biodiversity and Ecosystem Risk Assessment*, **7**, 5–50.

Davis SC, Griffiths H, Holtum J, Saavedra AL, Long SP (2011) The evaluation of feedstocks in GCBB continues with a special issue on agave for bioenergy. *GCB Bioenergy*, **3**, 1–3.

EIA (2013) *International Energy Outlook 2013*. EIA, Washington, DC.

Ellenberg H (1981) Ursachen des Vorkommens und Fehlens von Sukkulenten in den Trockengebieten der Erde. (Reasons for stem succulents being present or absent in the arid regions of the world). *Flora*, **171**, 114–169.

Escamilla-Treviño LL (2011) Potential of plants from the genus *Agave* as bioenergy crops. *BioEnergy Research*, **5**, 1–9.

ESRI (2012) ArcGIS Version 10.0. *ESRI (Environmental Systems Research Institute)*.

FAO, IIASA, ISRIC, ISSCAS, JRC (2012) Harmonised World Soil Database. *Harmonised World Soil Database (version1.2)*.

Garcia-Moya E, Romero-Manzanares A, Nobel PS (2011) Highlights for *Agave* productivity. *GCB Bioenergy*, **3**, 4–14.

GBEP (2011) *The Global Bioenergy Partnership Sustainability Indicators for Bioenergy*. Food and Agriculture Organization, UN., Rome, Italy.

Godfray HCJ, Beddington JR, Crute IR *et al.* (2010) Food security: the challenge of feeding 9 billion people. *Science*, **327**, 812–818.

Gracia de Cortazar V, Nobel PS (1990) Worldwide environmental productivity indices and yield predictions for a CAM plant, *Opuntia ficus-indica*, including effects of doubled $CO_2$. *Agricultural and Forest Meteorology*, **49**, 261–279.

Grams TEE, Borland AM, Roberts A, Griffiths H, Beck F, Lüttge U, Darmstadt TH (1997) On the mechanism of reinitiation of endogenous crassulacean acid metabolism rhythm by temperature changes. *Plant Physiology*, **113**, 1309–1317.

Holtum JAM, Winter K (2014) Limited photosynthetic plasticity in the leaf succulent CAM plant *Agave angustifolia* grown at different temperatures. *Functional Plant Biology*, **41**, 843–849.

Howells M, Hermann S, Welsch M *et al.* (2013) Integrated analysis of climate change, land-use, energy and water strategies. *Nature Climate Change*, **3**, 621–626.

IEA (2013) *World Energy Outlook 2013*.

Immerzeel DJ, Verweij PA, van der Hilst F, Faaaij APC (2014) Biodiversity impacts of bioenergy crop production: a state-of-the-art review. *GCB Bioenergy*, **6**, 183–209.

IPCC (2013) Climate Change 2013: The Physical Science Basis. *Contribution of Working Group I to the Fifth Assessment Report of the Intergovernmental Panel on Climate Change* (eds Stocker TF, Qin D, Plattner GK, Tignor M, Allen SK, Boschung J, Nauels A, Xia Y, Bex V, Midgley PM). Cambridge University Press, Cambridge, UK.

Kang S, Nair SS, Kline KL *et al.* (2014) Global simulation of bioenergy crop productivity: analytical framework and case study for switchgrass. *GCB Bioenergy*, **6**, 14–25.

Keshwani DR, Cheng JJ (2009) Switchgrass for bioethanol and other value-added applications: a review. *Bioresource Technology*, **100**, 1515–1523.

Kliemchen A, Schomburg M, Galla H, Lüttge U, Kluge M (1993) Phenotypic changes in the fluidity of the tonoplast membrane of crassulacean-acid-metabolism plants in response to temperature and salinity stress. *Planta*, **189**, 403–409.

Li H, Foston MB, Kumar R *et al*. (2012) Chemical composition and characterization of cellulose for *Agave* as a fast-growing, drought-tolerant biofuels feedstock. *RSC Advances*, **2**, 4951.

Medina E, Osmond CB (1981) Temperature dependence of dark $CO_2$ fixation and acid accumulation in *Kalanchoe diagremontiana*. *Australian Journal of Plant Physiology*, **8**, 641–649.

Nachtergaele F, Petri M (2008) *LADA: Mapping Land Use Systems at global and regional scales for Land Degradation Assessment Analysis, Version 1.1*.

NASA (2014) NASA Atmospheric Science Data Center. *Surface meteorology and solar energy*.

Nimmo HG (2000) The regulation of *phosphoenolpyruvate carboxylase* in CAM plants. *Trends in Plant Science*, **5**, 75–80.

Nobel PS (1976) Water relations and photosynthesis of a desert CAM plant, *Agave deserti*. *Plant Physiology*, **58**, 576–582.

Nobel PS (1988) *Environmental Biology of Agaves and Cacti*. Cambridge University Press, Cambridge, UK.

Nobel PS (1989) Nutrient index quantifying productivity of *Agaves* and *Cacti*. *Journal of Applied Ecology*, **26**, 635–645.

Nobel PS (1991) Tansley review No. 32 achievable productivities of certain CAM plants: basis for high values compared with C3 and C4 plants. *New Phytologist*, **119**, 183–205.

Nobel PS, Hartsock TL (1978) Resistance analysis of nocturnal carbon dioxide uptake by a crassulacean acid metabolism succulent, *Agave deserti*. *Plant Physiology*, **61**, 510–514.

Nobel PS, Hartsock TL (1983) Relationships between photosynthetically active radiation, nocturnal acid accumulation, and $CO_2$ uptake for a crassulacean acid metabolism plant, *Opuntia ficus-indica*. *Plant Physiology*, **7**, 71–75.

Nobel PS, Israel AA (1994) Cladode development, environmental responses of $CO_2$ uptake, and productivity for *Opuntia ficus-indica* under elevated $CO_2$. *Journal of Experimental Botany*, **45**, 295–303.

Nobel PS, De la Barrera E (2003) Tolerances and acclimation to low and high temperatures for cladodes, fruits and roots of a widely cultivated cactus, *Opuntia ficus-indica*. *New Phytologist*, **157**, 271–279.

Nobel PS, Meyer SE (1985) Field productivity of a CAM plant, *Agave salmiana*, estimated using daily acidity changes under various environmental conditions. *Physiologia Plantarum*, **65**, 397–404.

Nobel PS, Quero E (1986) Environmental productivity indices for a Chihuahuan Desert CAM plant: *Agave Lechuguilla*. *Ecology*, **67**, 1–11.

Nobel PS, Valenzuela AG (1987) Environmental responses and productivity of the CAM plant, *Agave tequilana*. *Agricultural and Forest Meteorology*, **39**, 319–334.

Nobel PS, Garcia-Moya E, Quero E (1992) High annual productivity of *Agaves* and *Cacti* under cultivation. *Plant, Cell and Environment*, **15**, 329–335.

Ogburn RM, Edwards EJ (2010) The ecological water-use strategies of succulent plants. In: *Advances in Botanical Research*, Vol. 55 (eds Kader J-C, Delseny M). pp. 179–225. Academic Press, Burlington.

Osmond CB (1978) Crassulacean acid metabolism: a curiosity in context. *Plant Physiology*, **29**, 379–414.

Owen NA, Griffiths H (2014) Marginal land bioethanol yield potential of four crassulacean acid metabolism candidates (*Agave fourcroydes*, *Agave salmiana*, *Agave tequilana* and *Opuntia ficus-indica*) in Australia. *GCB Bioenergy*, **6**, 687–703.

Van Renssen S (2011) A biofuel conundrum. *Nature Climate Change*, **1**, 389–390.

RSB (2013) RSB Principles & Criteria for Sustainable Biofuel Production. *RSB-STD-01-001 (Version 2.1)*, 1–29.

Sanderson MA, Reed RL, Mclaughlin SB *et al*. (1996) Switchgrass as a sustainable bioenergy crop. *Bioresource Technology*, **56**, 83–93.

Saxton KE, Rawls WJ, Romberger JS, Papendick RI (1986) Estimating generalized soil-water characteristics from texture. *Soil Science Society America Journal*, **50**, 1031–1036.

Scarlat N, Dallemand JF (2011) Recent developments of biofuels/bioenergy sustainability certification: a global overview. *Energy Policy*, **39**, 1630–1646.

Skinner RH, Adler PR (2010) Carbon dioxide and water fluxes from switchgrass managed for bioenergy production. *Agriculture, Ecosystems & Environment*, **138**, 257–264.

Slade R, Bauen A, Gross R (2014) Global bioenergy resources. *Nature Climate Change*, **4**, 99–105.

Smith JAC, Nobel PS (1986) Water movement and storage in a desert succulent: anatomy and rehydration kinetics for leaves of *Agave deserti*. *Journal of Experimental Botany*, **37**, 1044–1053.

Somerville C, Youngs H, Taylor C, Davis SC, Long SP (2010) Feedstocks for lignocellulosic biofuels. *Science*, **329**, 790–792.

Sperry JS, Hacke UG (2002) Desert shrub water relations with respect to soil characteristics and plant functional type. *Functional Ecology*, **16**, 367–378.

Stintzing FC, Carle R (2005) Cactus stems (*Opuntia* spp.): a review on their chemistry, technology, and uses. *Molecular Nutrition & Food Research*, **49**, 175–194.

Tilman D, Socolow R, Foley JA *et al*. (2009) Beneficial biofuels — the food, energy, and environment trilemma. *Science*, **325**, 270–271.

Ting IP (1985) Crassulacean acid metabolism. *Plant Physiology*, **36**, 595–622.

Wheeler T, von Braun J (2013) Climate change impacts on global food security. *Science*, **341**, 508–513.

Winter K, Smith JAC (1996) Crassulacean Acid Metabolism: Biochemistry, Ecophysiology, and Evolution. *Berlin, etc. Ecological studies*, **114**, 427–436.

WorldClim (2014) WorldClim - Global Climate Data. *ERSI grids for Min. Temperature, Max. Temperature, and Precipitation 30 arc-seconds (~1 km)*.

Yan X, Tan DKY, Inderwildi OR, Smith JAC, King DA (2011) Life cycle energy and greenhouse gas analysis for *Agave*-derived bioethanol. *Energy & Environmental Science*, **4**, 3110–3121.

## Supporting Information

Additional Supporting Information may be found in the online version of this article:

**Data S1.** Harmonised world soil atlas (HWSD) and geospatial estimates of soil hydraulic properties.

**Data S2.** Food and agriculture organisation (FAO) land-use constraints used to define 'low-grade' lands.

**Data S3.** Viable low-grade land productivity potential under climate change: continent scale simulation data.

**Data S4.** Additional information for working with S5–S8 using ArcGIS software

**Data S5.** ASCII file for Fig. 1a (Simulated global productivity, *A. tequilana*).

**Data S6.** ASCII file for Fig. 1b (Simulated global productivity, *O. ficus-indica*).

**Data S7.** ASCII file for Fig. 6a (Simulated global VL yield, *A. tequilana*).

**Data S8**. ASCII file for Fig. 6b (Simulated global VL yield, *O. ficus-indica*).